J Physiol 591.12 (2013) pp 3063–3080

The Journal of Physiology

Excitability and the safety margin in human axons during hyperthermia

James Howells[1], Dirk Czesnik[2], Louise Trevillion[1] and David Burke[1]

[1] *Institute of Clinical Neurosciences, Royal Prince Alfred Hospital and The University of Sydney, Sydney, Australia*
[2] *Department of Clinical Neurophysiology, University Medical Center Göttingen, Georg-August-University Göttingen, Göttingen, Germany*

Key points

- In six healthy subjects, the excitability of both motor and sensory axons was altered during hyperthermia, lowering their safety margin.
- The results suggest that slow K^+ channels play a significant role in these changes in axonal excitability during hyperthermia.
- Inward rectification was reduced during hyperthermia, and the modelling suggests that the hyperpolarization-activated cation current, I_h, was reduced, thus hampering its ability to counter activity-dependent hyperpolarization.
- Hyperthermia lowers the safety margin for action potential generation and propagation. Differences in their responses to hyperthermia suggest that motor axons undergo conduction block more readily than sensory axons during fever, particularly when the safety margin is already impaired.

Abstract Hyperthermia challenges the nervous system's ability to transmit action potentials faithfully. Neuromuscular diseases, particularly those involving demyelination have an impaired safety margin for action potential generation and propagation, and symptoms are commonly accentuated by increases in temperature. The aim of this study was to examine the mechanisms responsible for reduced excitability during hyperthermia. Additionally, we sought to determine if motor and sensory axons differ in their propensity for conduction block during hyperthermia. Recordings of axonal excitability were performed at normal temperatures and during focal hyperthermia for motor and sensory axons in six healthy subjects. There were clear changes in excitability during hyperthermia, with reduced superexcitability following an action potential, faster accommodation to long-lasting depolarization and *reduced* accommodation to hyperpolarization. A verified model of human motor and sensory axons was used to clarify the effects of hyperthermia. The hyperthermia-induced changes in excitability could be accounted for by increasing the modelled temperature by 6°C (and adjusting the maximum conductances and activation kinetics according to their Q_{10} values; producing a 2 mV hyperpolarization of resting membrane potential), further hyperpolarizing the voltage dependence of I_h (motor, 11 mV; sensory, 7 mV) and adding a small depolarizing current at the internode (motor, 20 pA; sensory, 30 pA). The modelling suggested that slow K^+ channels play a significant role in reducing axonal excitability during hyperthermia. The further hyperpolarization of the activation of I_h would limit its ability to counter the hyperpolarization produced by activity, thereby allowing conduction block to occur during hyperthermia.

J. Howells and D. Czesnik have contributed equally to this work as joint first authors.

DOI: 10.1113/jphysiol.2012.249060

(Received 26 November 2012; accepted after revision 18 April 2013; first published online 22 April 2013)
Corresponding author J. Howells: Level 2, Medical Foundation Building, K25, The University of Sydney, 92–94 Parramatta Rd, Camperdown 2050, N.S.W., Australia. Email: james.howells@sydney.edu.au

Abbreviations CMAP, compound muscle action potential; CSAP, compound sensory action potential; E_K, equilibrium potential for K^+ ions; HCN, hyperpolarization-activated cyclic nucleotide-gated channels; I_h, hyperpolarization-activated cation current; I-V, current-threshold relationship; K_f, fast potassium; K_s, slow potassium; Q_{10}, temperature coefficient over 10°C; QT, charge–duration relationship; RC, recovery cycle; RMP, resting membrane potential; RRP, relative refractory period; SDTC, strength–duration time constant; SR, stimulus–response relationship; TE, threshold electrotonus; TEd, depolarizing threshold electrotonus; TEh, hyperpolarizing threshold electrotonus; TEh100(260–300 ms), average threshold reduction, measured at 260–300 ms after the onset of a 100% hyperpolarizing conditioning current.

Introduction

Signalling in axons of the peripheral nervous system has long been known to be sensitive to temperature, and hyperthermia can impact on the ability of axons to faithfully transmit impulses to or from the peripheral nervous system. Cooling increases the duration and amplitude of an action potential and slows conduction velocity, and it has been suggested that this is primarily due to the slowing of Na^+ channel kinetics. Conversely, heating increases conduction velocity and decreases the response amplitude and duration of compound action potentials (Buchthal & Rosenfalck, 1966; Ludin & Beyeler, 1977; Rutkove *et al]*. 1997; Rutkove, 2001). In healthy individuals, the symptoms of fatigue and exhaustion can result from elevations in body temperature. In demyelinating disorders, increases in temperature can produce or exacerbate conduction block at sites of impairment of the safety margin for action potential generation. Experimentally demyelinated single nerve fibres may undergo reversible conduction block with elevations in nerve temperature as small as 0.5°C (Rasminsky, 1973). In a guinea-pig model of experimental allergic neuritis, Davis & colleagues (1975) found that the temperature for conduction block is a linear function of conduction velocity (which should be related to the degree of demyelination), confirming their earlier theoretical predictions (Schauf & Davis, 1974).

In the giant squid axon, Hodgkin & Katz (1949) found the resting membrane potential to be practically constant between 3 and 20°C, and then gradually depolarized by 10 to 15 mV up to 35°C. In contrast, they found the shape of an action potential to be much more affected by temperature. The temperature dependence of the falling phase of the action potential was much greater than of the rising phase, for which they postulated that different mechanisms were responsible. To account for the temperature dependence of ion channel gating, Hodgkin & Huxley (1952*a*,*b*) adopted a temperature coefficient (Q_{10}) of 3 for all rate constants. However, subsequent studies in myelinated fibres found Na^+ activation to be less temperature sensitive, with a Q_{10} of ∼2 (Frankenhaeuser & Moore, 1963, frog; Schwarz & Eikhof, 1987, rat). To a lesser extent, ion concentrations, Nernst potentials, ion channel permeability, axonal membrane capacity and axoplasmic resistance are also dependent on temperature (Hodgkin *et al.* 1952; Taylor & Chandler, 1962; Frankenhaeuser & Moore, 1963; Palti & Adelman, 1969).

In vivo threshold tracking techniques have been used to examine the underlying mechanisms of excitability in healthy and diseased human axons (Bostock *et al.* 1998; Kiernan *et al.* 2000; Krishnan *et al.* 2009). Cooling has a marked effect on the excitability of both motor axons and cutaneous afferents (Burke *et al.* 1999; Moldovan & Krarup, 2004) and even modest changes in temperature can have significant effects (Kiernan *et al.* 2001*a*). However, to date the effects of hyperthermia on axonal excitability in human subjects have not been studied, so that the responses of the nervous system during hyperthermia have to be inferred, primarily from studies of cooling.

In the present study, we examined the factors affecting the excitability of peripheral nerve axons when subjected to physiologically high temperatures. We find that slow potassium (K_s) channels contribute to a dampening of excitability at elevated temperatures, and that this is particularly evident during the recovery of excitability following an action potential. In addition, our modelling suggests that the voltage dependence of the hyperpolarization-activated current (I_h) is further hyperpolarized during hyperthermia. This would limit its ability to counter activity-dependent hyperpolarization and restore resting membrane potential (RMP). These changes would impact on the safety margin for action potential generation, and are likely to be factors in the conduction failure and fatigue of febrile illnesses, particularly in patients with diseases affecting axonal function, both central and peripheral.

Methods

The research followed the guidelines in the *Declaration of Helsinki* and ethics approval for the studies was obtained from the Human Research Ethics Committee of The University of Sydney, Australia. Experiments were performed on 27 separate occasions on six healthy subjects, all of whom provided written informed consent prior to the commencement of the study.

On each occasion we measured axonal excitability using the extended Trond protocol (Tomlinson *et al.* 2010; Howells *et al.* 2012) and a new protocol for studying polarized recovery cycles, first at a normal skin-surface temperature and then during focal hyperthermia. Sensory and motor axons of the median nerve of the six subjects were studied on separate occasions. To test the reproducibility of the results *within subjects*, measurements at normal temperature and during focal hyperthermia were performed on motor axons five times on separate days in two of the six subjects (subjects 1 and 2). The repeatability data for each subject were averaged before inclusion in the group data. The variability *within an experiment* was also tested five times in two subjects (subjects 2 and 3). Temperature was measured continuously near the site of stimulation using a skin-surface thermistor (YSI-409B; YSI Inc., Yellow Springs, OH, USA; see Fig. 1). Reusable 'click-style' sodium acetate heat pads (Maverick Co., Christchurch, New Zealand) were applied to the dorsal and palmar aspects of the distal forearm and hand to create focal hyperthermia at the site of stimulation, while the whole arm was wrapped in a blanket to slow temperature loss. The average skin surface temperatures recorded under control conditions were $32.5 \pm 0.2^{\circ}$C (mean $\pm$ SEM) for motor axons and $32.6 \pm 0.1^{\circ}$C for sensory axons. The temperatures recorded during heating ranged from 39.4 to 43.4°C. After application of the heat pads, measurements began within 5 min, when the skin-surface temperature had stabilized at its peak value ($41.7 \pm 0.1^{\circ}$C, mean $\pm$ SEM). Over the course of the experiment the mean temperature cooled slightly to $40.8 \pm 0.1^{\circ}$C, with a maximal drop in any experiment of 2.5°C.

Nerve excitability studies were performed using the QtracS software (© Hugh Bostock, Institute of Neurology, UCL, Queen Square, London, UK). Stimuli were applied to the median nerve at the wrist via non-polarizable Ag–AgCl adhesive electrodes (Cleartrace REF 1700–050, ConMed, Utica, NY, USA), with the anode placed 10 cm proximally on the radial edge of the forearm (see Fig. 1). Compound muscle action potentials (CMAPs) were recorded using the same Ag–AgCl electrodes with the active electrode over the thenar eminence, the reference electrode distally on the proximal phalanx of the thumb. Compound sensory action potentials (CSAPs) were recorded with disposable Ag–AgCl ring electrodes (RE-D; Electrode Store, EnumClaw, WA, USA) on digit 2 with the active electrode on the proximal phalanx, the reference approximately 4 cm distally. A ground electrode on the palm was used for both motor and sensory recordings. All electrodes were further secured to the skin with surgical tape (Transpore; 3M, St Paul, MN, USA) prior to commencement of the experiments.

A purpose-built isolated preamplifier with high common-mode rejection and low noise was used to amplify the compound action potentials (CMAP $\times$200; CSAP $\times$ 10,000) which then had mains-frequency noise removed with a HumBug Noise Eliminator (Quest Scientific, North Vancouver, BC, Canada) before being digitized by a data acquisition system (PCI-6221; National Instruments, Austin, TX, USA). QtracS and the data acquisition system provided the command signal for the delivery of stimuli by an isolated linear bipolar current stimulator (DS5; Digitimer, Welwyn Garden City, UK).

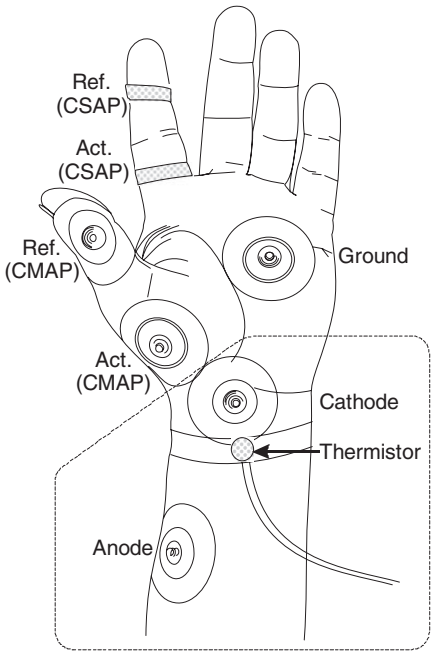

Figure 1. Recording arrangement
Stimuli were delivered at the wrist (cathode) using Ag–AgCl electrodes with the anode 10 cm distal on radial edge of the forearm. CMAPs were recorded over the thenar eminence, with the reference electrode on the proximal phalanx of the thumb. CSAPs were recorded using disposable Ag–AgCl ring electrodes on digit 2. The same ground was used for both motor and sensory recordings. Reusable 'click-style' sodium acetate heat pads were applied to the dorsal and palmar aspects of the distal forearm and hand, at wrist level (as indicated by the dotted lines), and the thermistor recorded the temperature close to the site of stimulation.

Excitability protocols

Excitability studies adjust the intensity of a test stimulus to track a constant fraction of the maximal compound action potential (target potential). The response to graded stimuli was measured first to determine stimulus–response (SR) properties, the size of the target potential and to optimize the tracking. For both motor and sensory studies, 1 ms-wide test stimuli were used, allowing simpler comparisons between motor and sensory axons and the use of strong hyperpolarization in sensory axons (Tomlinson *et al.* 2010; Howells *et al.* 2012). From the SR relationship, the target response was set to 50% of the maximal response (near the steepest part of the curve).

Routine axonal excitability assessment. The extended nerve excitability protocol (TrondNF) was used to study the excitability of axons at normal and hyperthermic temperatures. This protocol consists of five parts: stimulus–response relationship (SR; described above); strength–duration properties, which are plotted as charge *versus* duration (QT); threshold electrotonus (TE); current–threshold relationship (I-V; the threshold analogue of current-voltage) and the recovery cycle (RC).

The *strength–duration properties* of motor axons were studied by tracking the 50% target potential using stimuli of different widths: 1, 0.8, 0.6, 0.4 and 0.2 ms. There is a linear relationship between stimulus charge (stimulus strength × width) and stimulus width, with the slope and negative intercept on the *x*-axis representing rheobase and the strength–duration time constant (SDTC), respectively (Mogyoros *et al.* 1996). The strength–duration properties of sensory axons were made using narrower test widths (0.5, 0.4, 0.3, 0.2 and 0.1) to avoid dispersion of the CSAP that occurs with longer stimuli.

Threshold electrotonus was tested before, during and after long subthreshold conditioning currents. In addition to the standard conditioning currents of ±20 and ±40% of the unconditioned threshold (see Kiernan *et al.* 2000), two additional levels of hyperpolarization were included: a 200 ms-long hyperpolarizing current which was 70% of the control threshold, and a 300 ms long hyperpolarizing current which was 100% of the control threshold (Tomlinson *et al.* 2010; Howells *et al.* 2012).

The *current–threshold relationship* quantifies the rectifying conductances, both inward and outward, and the resting input conductance. The test threshold was measured at the end of a 200 ms conditioning current for 16 conditioning strengths from +50% (depolarizing) to −100% (hyperpolarizing) in 10% increments.

The *recovery cycle* measures the recovery of excitability following supramaximal stimulation at 18 conditioning–test intervals which change in a logarithmic fashion between 2 and 200 ms. Under normal conditions axons undergo a distinct pattern of excitability following an action potential (Adrian & Lucas, 1912). Initially the axons are inexcitable (absolute refractoriness), followed by reduced excitability (relative refractoriness), the end of which corresponds to the relative refractory period (RRP). After refractoriness axons undergo a period of superexcitability which is associated with the depolarizing afterpotential (Barrett & Barrett, 1982), and then a period of subexcitability ensues, attributed to the after-hyperpolarization.

Polarized recovery cycles. To determine whether changes in membrane potential contribute to the changes in the recovery cycle much as described in Bergmans (1970) and Kiernan & Bostock (2000), recovery cycles were measured in the same way as described above, at rest and during background polarization, at normal and hyperthermic temperatures. The recovery cycle was measured 200 ms after the onset of long +30% (depolarizing) and −30% (hyperpolarizing) currents which extended beyond the test stimulus.

Mathematical modelling

The Bostock model of the human motor axon (Bostock *et al.* 1991), as modified by Howells and colleagues (2012) for motor and sensory axons, was used to assist in the interpretation of the excitability changes during focal hyperthermia. This space-clamped model is well suited to the simulation of superficially located nerves stimulated with relatively large electrodes, and has been used to model the changes in axonal excitability in tetrodotoxin poisoning (Kiernan *et al.* 2005), porphyria (Lin *et al.* 2008), and following stroke and multiple sclerosis (Jankelowitz *et al.* 2007; Ng *et al.* 2008). The model consists of nodal and internodal compartments, which are linked by the Barrett–Barrett conductance, representing paranodal pathways through and under the myelin sheath (Barrett & Barrett, 1982; Mierzwa *et al.* 2010). To model the effects of focal hyperthermia on axonal excitability, the ion channel rate constants were increased according to their Q_{10} values (Hodgkin & Huxley, 1952*a*,*b*; Frankenhaeuser & Moore, 1963; Guttman, 1971; Hart, 1983; Schwarz & Eikhof, 1987): Na^+ activation 'm', 2.2; Na^+ inactivation 'h', 2.9; K^+ (fast and slow) and HCN channels, 3. As the maximal conductances are affected by changes in passive diffusion, a Q_{10} of 1.4 was also applied to all voltage-gated ion channel (Hodgkin & Huxley, 1952*a*,*b*; Moore, 1958; Hart, 1983; Hille, 1992), leak and Barrett–Barrett conductances. The effect of temperature on capacitance is negligible (Hodgkin *et al.* 1952; Tasaki, 1955;

Table 1. Axonal excitability measures at normal and hyperthermic temperatures

	Motor			Sensory		
	Normal	Hyper.	*P* value	Normal	Hyper.	*P* value
Latency to peak (ms)	6.4 (0.3)	6.1 (0.2)	0.02	3.2 (0.1)**	3.1 (0.1)**	0.003
Peak response (mV, μV)*	6.4 [1.22]	6.0 [1.21]	0.24	40.0 [1.16]	46.5 [1.19]	0.12
Stim for 50% max (mA)	4.3 (0.4)	5.1 (0.6)	0.16	3.6 (0.6)	3.9 (0.5)	1
Rheobase (mA)	2.8 (0.3)	3.4 (0.4)	0.20	2.2 (0.3)	2.7 (0.4)	0.6
SR slope*	4.33 [1.09]	4.11 [1.07]	1	1.59 [1.11]	1.70 [1.10]	0.5
SDTC (μs)	517 (54)	506 (30)	0.7	724 (128)	648 (47)	0.8
TEd40(peak) (%)	66.4 (2.0)	61.9 (2.1)	0.003	60.3 (1.7)	57.7 (1.5)	0.26
Accomm. half-time (ms)	38.2 (0.7)	29.6 (0.5)	0.004	38.0 (1.9)	31.6 (0.7)	0.2
TEd40(undershoot) (%)	−19.5 (1.4)	−10.6 (1.1)	0.007	−17.7 (0.8)	−11.4 (0.6)	0.01
TEd20(peak) (%)	38.0 (1.4)	35.8 (1.7)	0.005	33.0 (0.9)	31.4 (0.9)	0.33
TEd20(undershoot) (%)	−10.5 (0.7)	−4.9 (0.7)	0.006	−9.0 (0.5)	−6.6 (0.7)	0.28
TEh20(overshoot) (%)	8.8 (0.8)	4.0 (0.9)	0.006	7.0 (0.3)	4.9 (0.3)	0.04
TEh40(overshoot) (%)	15.8 (1.4)	7.0 (1.2)	0.005	12.1 (0.5)	7.4 (0.4)	0.005
TEh100(260–300 ms) (%)	−334 (33)	−366 (37)	0.02	−270 (13)	−292 (11)	0.03
Resting *I–V* slope	0.61 (0.04)	0.59 (0.06)	0.4	0.71 (0.02)	0.69 (0.03)	0.5
Hyperpol. *I–V* slope	0.33 (.03)	0.31 (0.02)	0.6	0.31 (0.02)	0.33 (0.02)	1
Refract. at 2 ms (%)	64.0 (15.7)	20.0 (8.0)	0.02	46.5 (9.4)	24.3 (4.1)	0.02
RRP (ms)*	3.1 [1.08]	2.5 [1.08]	0.04	3.1 [1.09]	2.9 [1.07]	0.02
Superexcit. area (% ms)	−140 (27)	−35 (15)	0.006	−116 (24)	−39 (13)	0.008
Subexcit. area (% ms)	1124 (142)	952 (284)	0.45	767 (49)	633 (161)	0.50

Values are presented as mean and SEM (in parentheses). *P* values are from Student *t* tests of paired data. Related measures, as indicated by parentheses, were corrected for multiple comparisons using the Holm-Bonferroni method. *These measures are normally plotted on a logarithmic scale and are reported as the geometric mean and SEM (in square brackets, as a factor). **Sensory latencies using a 0.5 ms-wide test stimulus.

Taylor & Chandler, 1962; Palti & Adelman, 1969), and capacitances in the model were therefore not adjusted for hyperthermia.

Statistical analysis

Group data are reported as mean (and SEM), except for measures that are better plotted on logarithmic scales to be normally distributed. Here geometric means were calculated and reported as mean [geometric SEM (as a factor)] (Kiernan *et al.* 2000). The mean values for the two groups (normal and hyperthermic) were compared with Student's *t* tests for paired data, and are reported in Table 1. The *P* values of related measures (as indicated by the parentheses in Table 1) were adjusted for multiple comparisons using the Holm-Bonferroni method, and the corrected values are reported in the text and Tables.

For statistical analysis the extent of superexcitability was measured as the area below the *x*-axis following the relative refractory period. Similarly, the extent of subexcitability (which follows superexcitability) was measured as the area above the *x*-axis.

Results

CMAP recruitment

The latency from the onset of the test stimulus to the peak of the CMAP was 0.36 ms shorter when hyperthermic ($P < 0.02$), though the amplitude of the peak CMAP recorded at the normal and hyperthermic temperatures was not significantly different ($P = 0.24$; Fig. 2*A* and Table 1). The stimulus current required for a half-maximal response and rheobase were both higher during hyperthermia but not significantly so after adjustment for multiple comparisons (respectively, 5.1 ± 0.6 mA (hyperthermia) and 4.3 ± 0.4 mA (normal) and 3.4 ± 0.4 mA (hyperthermia) and 2.8 ± 0.3 mA (normal); see Fig. 2*A* (large circles), and *B* and Table 1). The stimulus–response slopes and strength–duration time constants were also not significantly different (see Fig. 2*C* and Table 1).

Threshold electrotonus and current–threshold relationship in motor axons

Accommodation to depolarizing currents was more rapid during hyperthermia than at normal temperatures (see Fig. 3*A*), such that the maximal threshold reduction was less (with +40%: 61.9 ± 2.1% and 66.4 ± 2%, respectively; with +20%: 35.8 ± 1.7% and 38 ± 1.4%, respectively; see Table 1) and accommodation half-time was shorter (the time to the midpoint between the peak threshold reduction and the average level at the end of the polarization; hyperthermia, 29.6 ms; normal, 38.2 ms; see Table 1). The undershoot after the 100 ms depolarizing current ended is due to the slow de-activation of accommodative conductances active at the end of the depolarization; the peak undershoot occurred earlier but was smaller for both levels of polarization during hyperthermia ($P \leq 0.007$; see Table 1).

In contrast, significant differences in the accommodation to hyperpolarization were only apparent for the strongest hyperpolarizing current and during the hyperpolarizing overshoots (see Fig. 3*B* and Table 1). Unexpectedly, the accommodation appeared slower during hyperthermia, and excitability was reduced at the end of the long −100% hyperpolarizing currents (i.e. at the intervals between 260 and 300 ms, 'TEh100(260–300 ms)'; $P = 0.02$).

Figure 3*C* shows the current–threshold relationship (a threshold analogue of current/voltage, '*I–V*', plots), measured at the end of a 200 ms-long conditioning current. Hyperthermia produced no significant differences in the resting and hyperpolarizing *I–V* slopes ($P = 0.4$ and 0.6, respectively; see Table 1).

The fact that the hyperpolarizing portion of the current–threshold relationship appears unaffected by hyperthermia is consistent with the equivalent data in threshold electrotonus (see ellipses and rectangles in Figs 3*B* and *C* and 6*B* and *C*), and probably reflects opposing effects on HCN channels which cancel each other out for all but the strongest and longest hyperpolarization (see Modelling and Discussion sections).

The recovery cycle of motor axons

The hyperthermia-induced changes in excitability of motor axons were particularly obvious in the recovery after a conditioning discharge (Fig. 3*D* and Table 1). The recordings during focal hyperthermia were characterized by less refractoriness at 2 ms (20 ± 8% and 64 ± 16%), a shorter relative refractory period (2.5 ± 0.2 ms and 3.1 ± 0.2 ms), with earlier superexcitability of reduced area (−35 ± 15% ms and −140 ± 27% ms). Similarly, subexcitability occurred earlier during hyperthermia but its area was not significantly different ($P = 0.45$).

Reproducibility

In order to demonstrate the reproducibility within single subjects, all measurements for motor axons were performed five times on separate days in two of the six subjects (subjects 1 and 2; the mean data for each of these two subjects were used in the group data averages). The individual recordings and mean data for one subject (subject 1) are shown in Fig. 4. The results were quite reproducible and comparable to the group data.

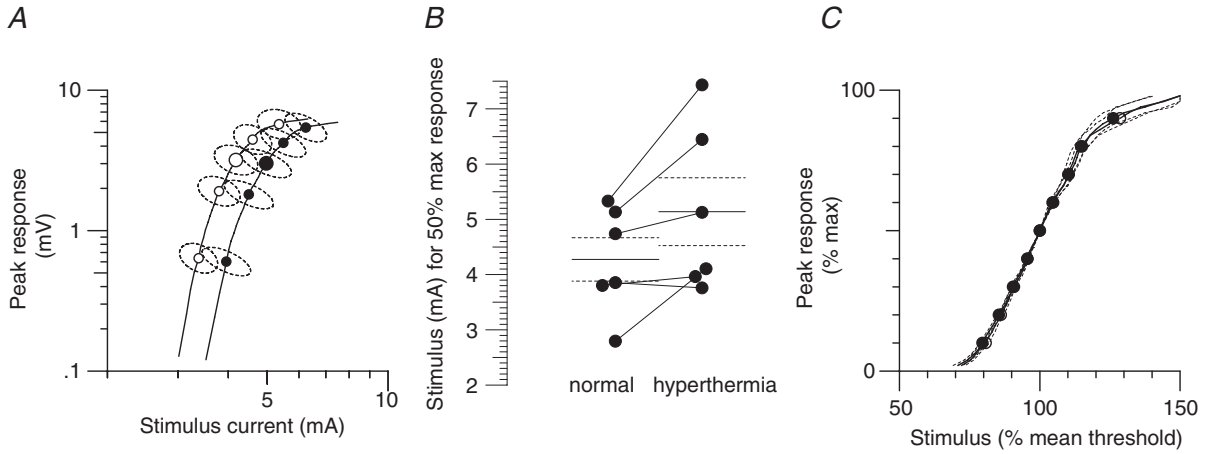

Figure 2. Stimulus–response relationship during hyperthermia
Group data ($n = 6$). *A*, recruitment of CMAP (measured baseline to peak) by gradually increasing stimulus intensity (normal temperature, open circles; hyperthermia, filled circles). *B*, stimulus required to recruit a half-maximal response at normal and hyperthermic temperatures. The continuous and dashed horizontal lines indicate the mean and standard errors (the mean half-maximal stimulus is also indicated by the large circles around the symbols in *A*.). *C*, normalized stimulus–response relationship recorded at normal and hyperthermic temperatures (open and closed circles, respectively). The peak response is normalized to a percentage of maximum and the stimulus is normalized to the stimulus current required for a half-maximal potential, before being averaged.

As is usually the case (Tomlinson *et al.* 2010; Howells *et al.* 2012), the greatest variability was seen for the strongest hyperpolarizing currents in threshold electrotonus (which is not surprising considering the number of possible modulators of hyperpolarization-activated cyclic nucleotide-gated (HCN) channels). To explore the source of variability further, repeated measurements were made five times in the same experiment in each of two subjects (subjects 2 and 3). Fig. 5 compares the variability within an experiment, within a subject and between all subjects, and these data are summarized in Table 2. The data shows that the variability within an experiment is considerably lower than within the same subject on different days. We expected an increase in excitability during hyperthermia. Based on the within-experiment variability a power analysis using TEh100(260–300 ms) indicated that with six subjects we were sufficiently powered (80%) to detect a 7.9% increase in excitability at $\alpha = 0.05$. The actual change during hyperthermia was much larger (32%), and in the opposite direction to that hypothesized. The variability *within* an experiment is the relevant measure for the present studies because the normal and hyperthermic studies were done within the *same* experiment.

Excitability of sensory axons

The hyperthermia-induced changes in sensory excitability are shown in Fig. 6 and are summarized in Table 1. These changes were qualitatively similar to those described above for motor axons with, in the recovery cycle (Fig. 6*D*), reduced refractoriness (24 ± 4% *vs.* 46 ± 9%), a shorter relative refractory period (2.9 ± 0.2 ms *vs.* 3.2 ± 0.3 ms), reduced superexcitability (−8.3 ± 2.4% *vs.* −17.6 ± 2.8%) and, in threshold electrotonus, reduced undershoot

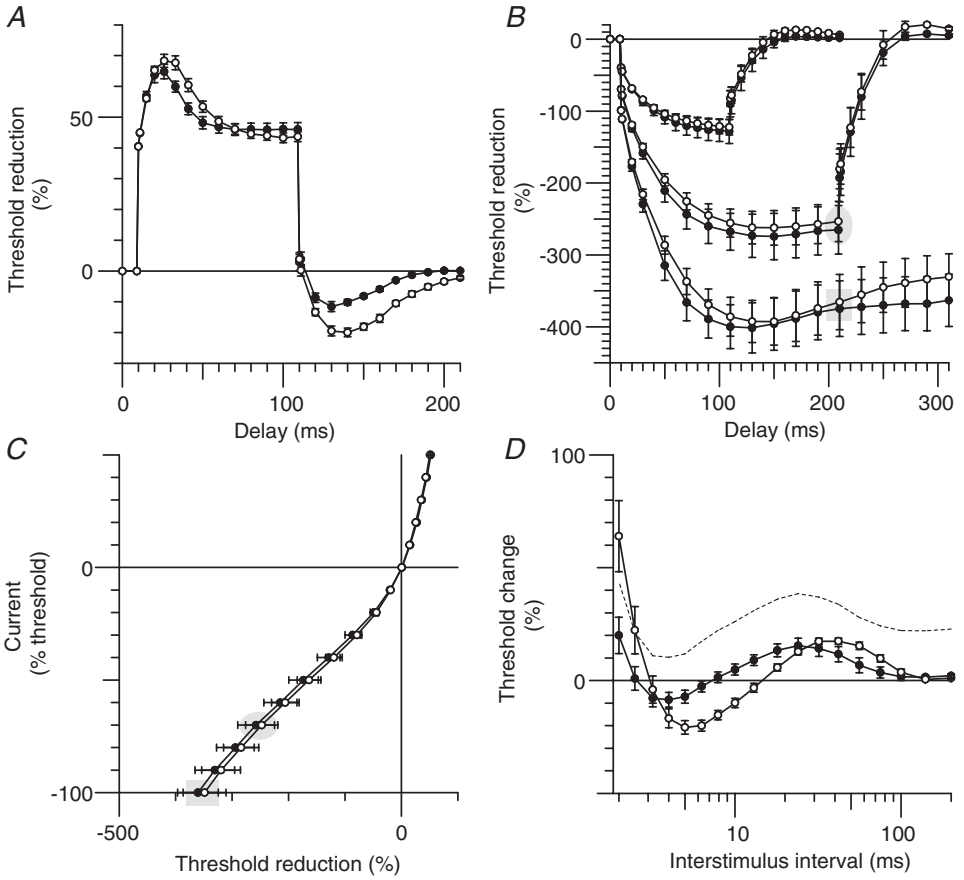

Figure 3. Motor axon excitability during focal hyperthermia
Group data ($n = 6$; mean ± SEM). Measurements of axonal excitability were made at normal resting temperature (open circles) and during focal hyperthermia (filled circles). *A*, threshold electrotonus for a depolarizing conditioning current of +40% of the unconditioned threshold. *B*, threshold electrotonus for hyperpolarizing conditioning currents of −40, −70 and −100%. *C*, current–threshold relationship for 200 ms-long conditioning currents from +50% (depolarizing) to −100% (hyperpolarizing) of the control threshold. *D*, the recovery of excitability following a supramaximal discharge. The dotted line represents the recovery of excitability during hyperthermia when normalized to the unconditioned threshold at 'normal' temperature (see Discussion). The corresponding data points in threshold electrotonus (*B*) and the current–threshold relationship (*C*) are highlighted by the shaded ellipses and rectangles for hyperpolarization by −70 and −100%, respectively.

(Fig. 6*A*; −11.4 ± 0.6% *vs.* −17.7 ± 0.8%) and overshoot (Fig. 6*B*; 7.4 ± 0.4% *vs.* 12.1 ± 0.5%). Hyperthermia had little effect on hyperpolarizing threshold electrotonus and the current–threshold relationship for sensory axons, except at the end of the strongest hyperpolarization of threshold electrotonus (Fig. 6*B*). The other measures showed trends in the same direction as with motor axons, but the changes were smaller and not significant.

Polarized recovery cycles

To examine the extent to which changes in membrane potential could contribute to the changes in the recovery cycle (the measure most distorted during hyperthermia), we made recordings while injecting depolarizing and hyperpolarizing currents to change membrane potential (Fig. 7). The effects of changes in temperature are

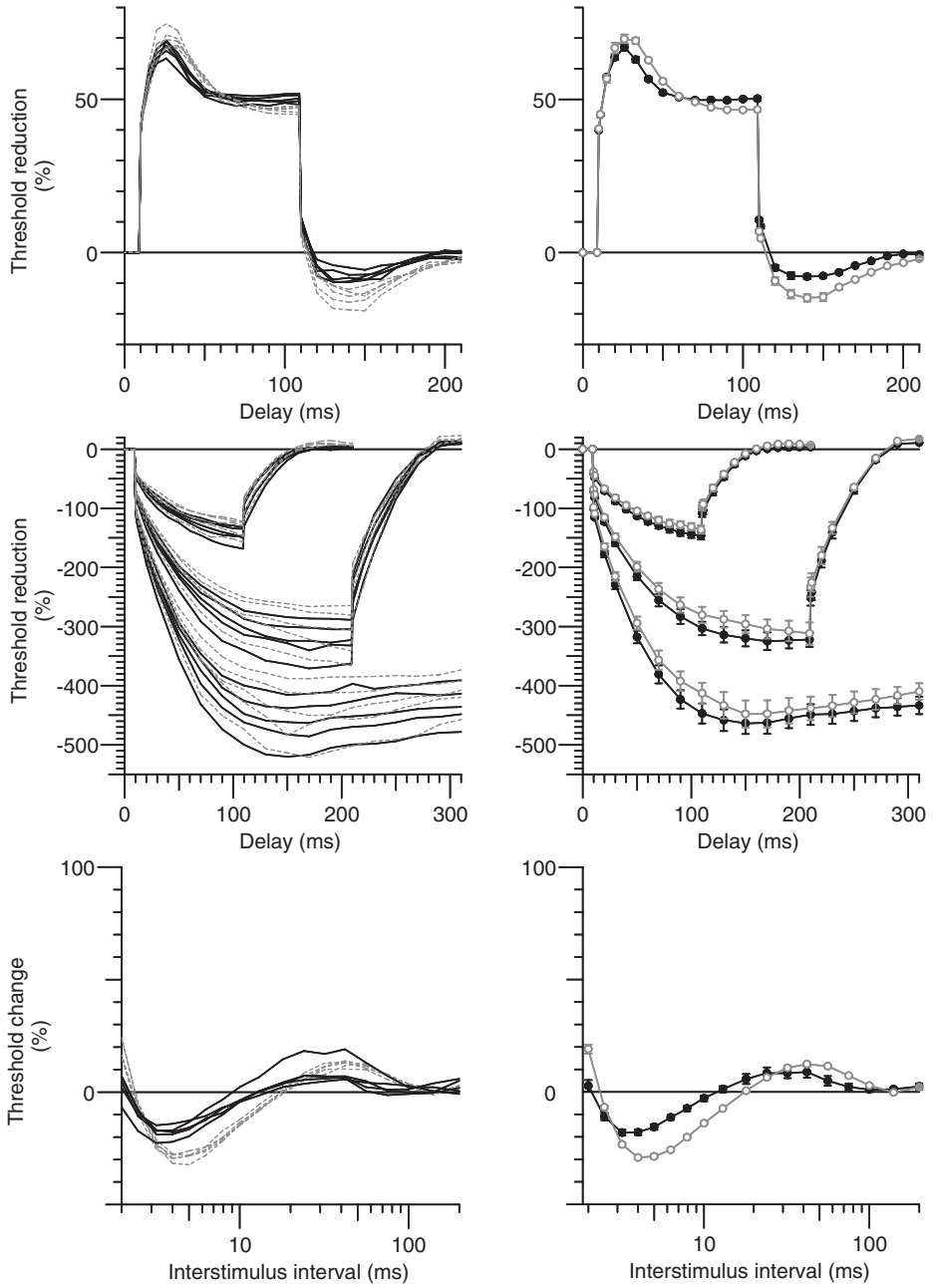

Figure 4. Reproducibility of hyperthermia induced changes
Left column, repeated measurements of axonal excitability in subject 1 on five separate occasions (normal temperature, dashed lines; hyperthermia, continuous lines). Right column, mean data (normal temperature, open circles; hyperthermia, filled circles; mean ± SEM). Top row, depolarizing threshold electrotonus (+40%; as in Fig. 2*A*). Middle row, hyperpolarizing threshold electrotonus (−40, −70 and −100%; as in Fig. 2*B*). Bottom row, recovery cycle.

generally explained by changes in Na^+ currents, but it is probable that an enhanced Na^+ current would produce a left-ward shift in the stimulus–response curve, rather than the trend for a shift to the right shown in Fig. 2*A*. The reduction in refractoriness could occur with hyperpolarization of RMP, but the reduced superexcitability and early accommodation in depolarizing threshold electrotonus favour depolarization. During depolarization (+30% threshold, approximately +1.2 mA for motor axons and 0.5 mA for sensory axons; triangles in Fig. 7) superexcitability was abolished in motor axons (Fig. 7*A*), and in five of the six subjects for sensory axons (Fig. 7*B*). The peak of subexcitability occurred earlier, as seen in hyperthermia ($P = 0.002$ for motor axons and $P = 0.04$ for sensory), but unlike hyperthermia, the extent of subexcitability was greater. These findings are similar to those of Kiernan & Bostock (2000). During hyperpolarization (–30% threshold, approximately −1.2 mA for motor axons and −0.5 mA for motor axons; squares in Fig. 7), the peak of superexcitability was larger and occurred at much the same conditioning-test intervals, while subexcitability was smaller and later. Hyperpolarization removes resting activation of K_s channels revealing recovery cycles that better represent the true extent of the decay of current through the Barrett–Barrett pathways (compare squares to circles in Fig. 7).

Data from recordings at the normal temperature and during hyperthermia (open and filled symbols, respectively, in Fig. 7) demonstrate that changes in membrane potential could not restore the normal recovery cycle during hyperthermia.

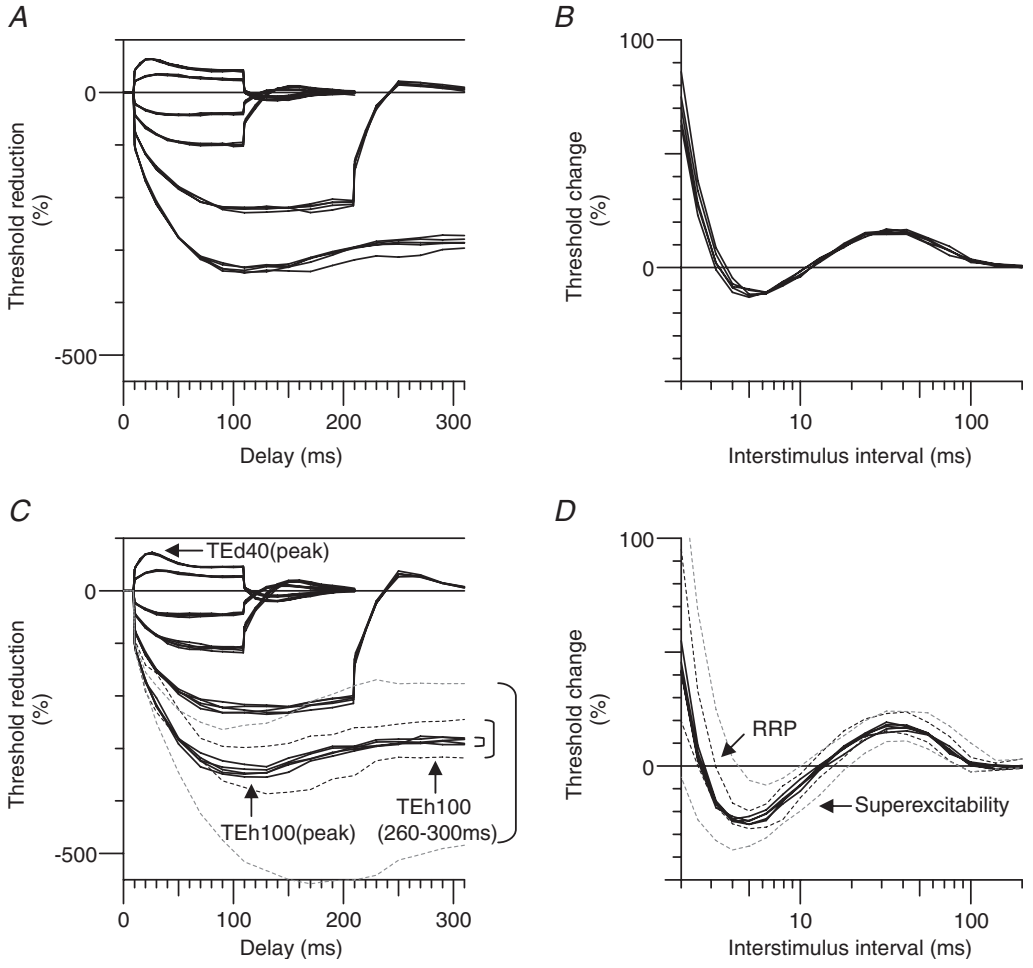

Figure 5. Reproducibility of excitability measures within an experiment
Five repeated measurements within the same experiment for subject 3 for threshold electrotonus (*A*) and the recovery cycle (*B*). Five repeated measurements (continuous lines) in subject 2 for threshold electrotonus (*C*) and the recovery cycle (*D*). The brackets in *C* highlight differences in the variability for the strongest hyperpolarization. The smallest bracket shows the within-experiment variability, the next largest bracket and the inner dashed lines indicate the within-subject variability (95% confidence limits) on different days, while the largest bracket and the outer dashed lines show the 95% confidence limits for all subjects. Note that the within-experiment variability is the measure relevant to the present studies.

Table 2. Variability of excitability measures in motor axons

	Same subject, within experiment	Same subject, different days	Between subjects ($n = 6$)
TEd40(peak) (%)	0.8 (1.1%)	1.4 (2.2%)	4.8 (7.3%)
TEh100(peak) (%)	8.2 (2.4%)	23 (6.8%)	79 (19.8%)
TEh100(260–300 ms) (%)	5.5 (1.9%)	18 (6.3%)	81 (24.1%)
RRP (ms; geometric SD)*	1.026	1.06	1.198
Superexcitability (%)	1.2 (5.2%)	1.5 (6.9%)	7.05 (35.8%)
Superexcit. area (% ms)	−12.5 (8.8%)	−16.4 (12.1%)	−65.4 (46.9%)

Figures are for the standard deviation and the coefficient of variation is in parentheses. *RRP – geometric standard deviation (as a factor).

Modelling

The Bostock model as modified by Howells and colleagues (2012) was used to interpret the hyperthermia-induced changes in motor and sensory axons. The average increase in skin surface temperature was 8.9°C, but the effects of hyperthermia were better modelled by an increase in nerve temperature of 6°C, the difference being an intuitively reasonable skin–nerve gradient during external heating. The rate constants of the gating processes in this model were increased according to the following Q_{10} values (Na^+ activation, 2.2; Na^+ inactivation, 2.9; fast K^+, slow

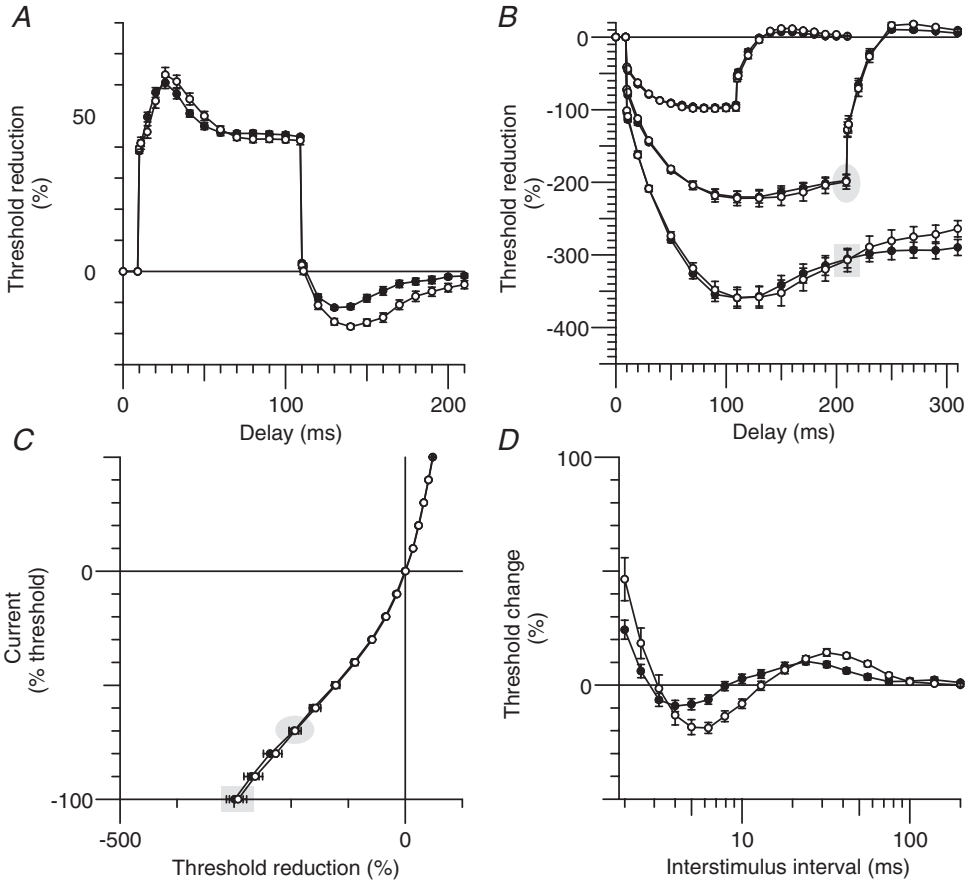

Figure 6. Sensory axon excitability during hyperthermia
Group data ($n = 6$, mean ± SEM), open circles represent measures at normal temperatures and filled circles during hyperthermia. *A*, depolarizing threshold electrotonus with a conditioning current of +40% of the control stimulus. *B*, hyperpolarizing threshold electrotonus with currents −40, −70 and −100% of the control stimulus. *C*, current–threshold relationship tested at the end of 200 ms long conditioning currents (−100% to 50% of control threshold). *D*, recovery cycle after supramaximal stimulation. The corresponding data points in threshold electrotonus (*B*) and the current–threshold relationship (*C*) are highlighted by the shaded ellipses and rectangles for hyperpolarization by −70 and −100%, respectively.

K^+, I_h activation, 3) and a Q_{10} of 1.4 was applied to all of the maximal conductances (i.e. all voltage-gated ion channels, leak conductances and the Barrett–Barrett pathways through and under the myelin sheath).

Motor axons. Increasing the temperature by 6°C lowered the potassium equilibrium potential (E_K; −94.8 mV from −93 mV), and this would have resulted in hyperpolarization of RMP by 1 mV. In combination with the increased conductances (particularly G_{Ks}), the resultant hyperpolarization of RMP was 1.7 mV.

The combined effect of hyperpolarization of E_K and RMP, faster gating and larger conductances modelled well most of the hyperthermia-induced changes in the recovery cycle, accurately replicating the earlier relatively refractory period, earlier and reduced superexcitability and earlier (though reduced) late subexcitability. However the lesser inward rectification during both strong and long hyperpolarization in threshold electrotonus and the current-threshold relationship could not be reproduced by these changes alone. The most parsimonious explanation for this unexpected and seemingly paradoxical finding is a reduction in I_h. Accordingly all parameters associated with I_h were varied, and the best fit was obtained with hyperpolarization of the half-activation voltage of I_h (by −11 mV). This additional change in gating has precedent, and its extent compares favourably with the reported temperature sensitivity of the voltage activation of the cardiac isoform (I_f) in sheep Purkinje fibres (Hart, 1983; −8 mV between 27.5 and 36.4°C; see Fig. 8*A* in that paper).

In addition, a constant (DC) *depolarizing* current of 20 pA at the internode improved the fit to hyperpolarizing threshold electrotonus, the current–threshold relationship and the recovery cycle during hyperthermia in motor axons (see Fig. 8). This depolarizing influence could reflect greater activity of slow internodally located HCN isoforms (see Howells *et al.* 2012), and its extent may actually be greater than 20 pA because Na^+–K^+ pump activity probably increases, at least transiently, with elevated temperatures. It must be acknowledged however, that this constant depolarizing current is an approximation and, if indeed it does represent slow HCN isoforms, then it is also true that the current through a voltage-gated ion channel should diminish as the membrane potential approaches the equilibrium potential for HCN channels. The modelling suggests that the electrochemical driving force for HCN channels varies threefold (and as a consequence the current through slowly gated channels) during threshold electrotonus and is ∼−23 mV for the 40% depolarization and ∼−77 mV at the peak of the strongest hyperpolarization (100%). This probably explains why a greater separation of the modelled normal and hyperthermic excitability exists at the end of the depolarizing threshold electrotonus (90–100 ms) than for the observed recordings (compare Figs 8*A* and 9*A* with Figs 3*A* and 6A, respectively). This apparent discrepancy provides further support for the possibility of slower isoforms of HCN channels on motor axons.

Sensory axons. Similarly the hyperthermia-induced changes in excitability were modelled well by an increase in temperature of 6°C, increased gating kinetics and maximal conductances (according to the Q_{10} values), hyperpolarization of the voltage dependence of I_h (by −7 mV) and a constant (DC) current of 30 pA (see Fig. 9). It is noteworthy that, when normothermic, the voltage dependence of I_h in motor axons is likely to be some 13 mV more hyperpolarized than that of sensory axons

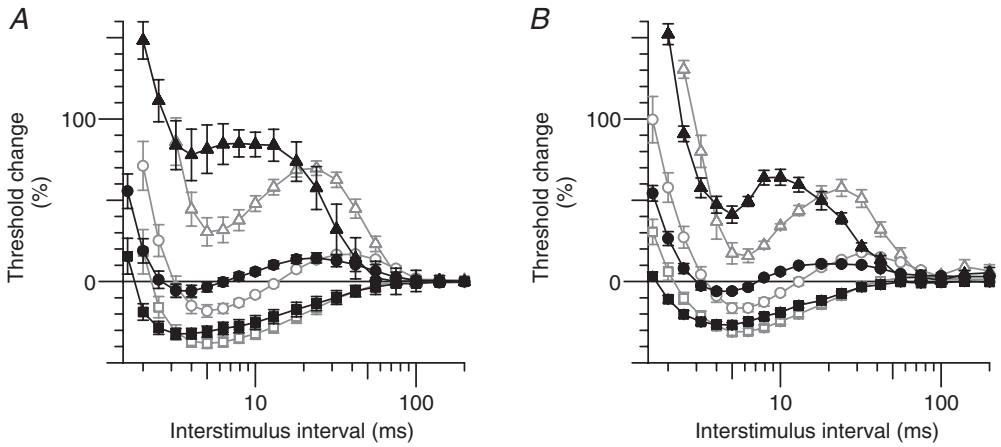

Figure 7. Polarized recovery cycles
Group data ($n = 6$; mean ± SEM). Recovery from activation during polarization (depolarization, triangles; hyperpolarization, squares) and without polarization (circles) at normal temperature (open symbols) and during hyperthermia (filled symbols). *A*, motor axons. *B*, sensory axons. The recovery cycle was measured 200 ms after the onset of a long conditioning pulse of strength 30% (depolarization; triangles) and −30% (hyperpolarization; squares) of the unconditioned test stimulus, respectively.

(Howells *et al.* 2012), and this discrepancy would increase to ∼17 mV during hyperthermia.

The effect of hyperthermia on inward rectification in sensory axons was only apparent during strong and long hyperpolarization. The modelled hyperpolarization of the voltage dependence of I_h was therefore nearly perfectly balanced with any increase in I_h due to increased diffusion or faster kinetics.

Discussion

We have studied for the first time the effects of focal hyperthermia on the excitability of human peripheral myelinated nerve. There are studies of nerve conduction during hyperthermia in human subjects (Rutkove *et al.* 1997), but studies of the effect of temperature on the excitability of human axons have focused on either cooling (Burke *et al.* 1999) or small deviations around normal temperature (Kiernan *et al.* 2001*a*; Maurer *et al.* 2010), while, in the cat, there have been comparable studies of axonal excitability only during cooling (Moldovan & Krarup, 2004).

The action potential of mammalian myelinated axons can be modelled adequately incorporating only Na^+ channels into the model (Schwarz *et al.* 1995), and the traditional view has been that the predominant effect of changes in temperature is likely to be due to changes in ion channel kinetics (Hodgkin & Huxley, 1952*b*; Schwarz & Eikhof, 1987; Burke *et al.* 1999; Kiernan *et al.* 2001*a*), and in particular those of Na^+ channels. This may be so for small changes in axonal temperature. While changes in Na^+ currents may well be the major factor shaping the action potential when temperature is close to normal, we suggest below that other currents exert a greater influence with marked increases in temperature. We suggest that these changes will reduce the safety margin for action

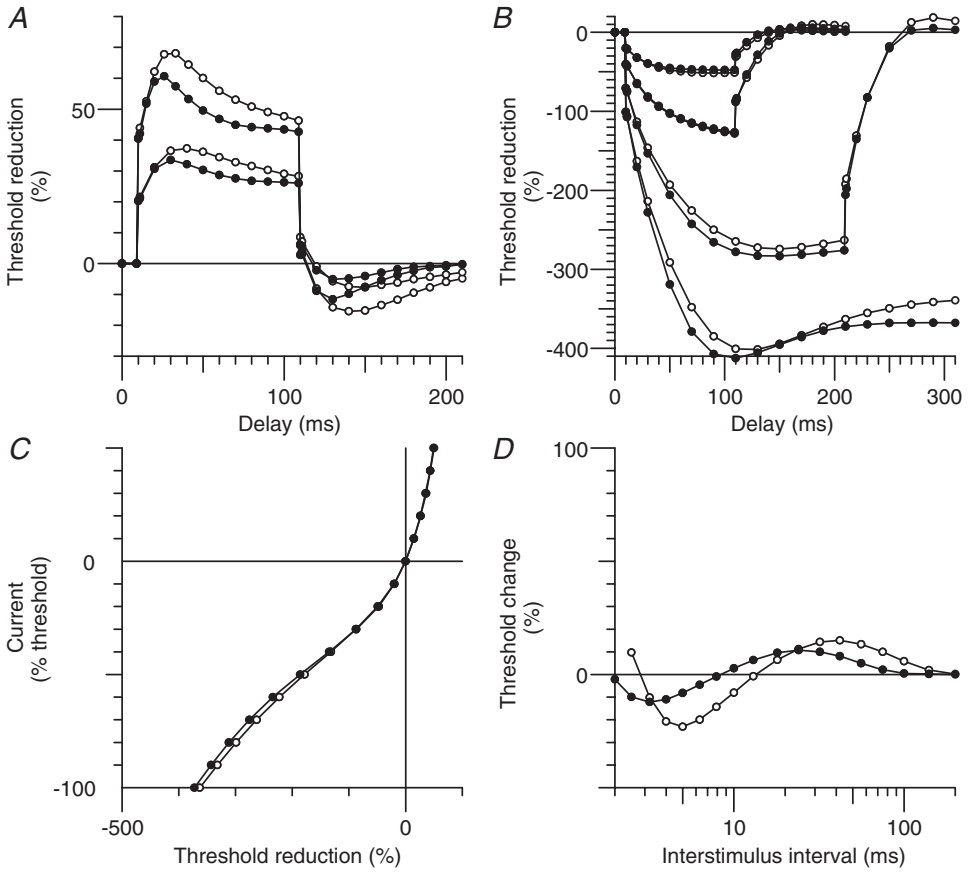

Figure 8. Mathematical model of the hyperthermia-induced changes in excitability of motor axons. The open circles indicate the Bostock motor axon model at normal temperature, and the modelled changes during hyperthermia are shown as closed circles. Hyperthermia was modelled by an increase in temperature of 6°C (with the activation kinetics and maximum conductances increased according to their respective Q_{10} values; see the Methods section), a hyperpolarization of the half-activation voltage of I_h (11 mV) and a small additional depolarizing current at the internode of 20 pA. *A*, depolarizing threshold electrotonus for +40% and +20% of the control threshold. *B*, hyperpolarizing threshold electrotonus (−20%, −40%, −70% and −100%). *C*, current–threshold relationship. *D*, the recovery of excitability after a supramaximal stimulus.

potential generation and propagation, and will do so more for motor axons than sensory axons, impairing conduction and leading to fatigue in normal subjects and, particularly, in patients with diseases affecting central and peripheral axons.

Mechanisms underlying hyperthermia-induced changes in excitability

Resting membrane potential. Kiernan & Bostock (2000) found the sensitivity of the threshold for the half-maximal CMAP to polarization to be ∼8% per millivolt, which when applied to the small increase in threshold during hyperthermia would suggest a hyperpolarization of 2.2 mV. Applying the same logic to the sensitivity of rheobase to changes in RMP gives a hyperpolarization of 2.1 mV. There is a dearth of literature on Na^+–K^+ pump functions in axons during heating, but a temperature-dependent increase in Na^+–K^+ pump activity could account for some of this hyperpolarization. Nevertheless our modelling suggests that the effects of temperature on the equilibrium potentials (in particular E_K) and on diffusion through channels open at rest are sufficient to account for 1.7 mV of hyperpolarization.

The hyperpolarization of RMP suggested by the modelling findings needs to be reconciled with the lack of a significant hyperpolarizing change in the threshold, rheobase and shift in the SR curve. These findings are not in conflict: the modelling suggested an offsetting tonic depolarization (which could be due to internodally located slow HCN isoforms) which would rein in the hyperpolarization of RMP to ∼0.6 mV. In any case, hyperpolarization by <2 mV is small, less than the range of holding potentials that result in inactivation of 30% Na^+

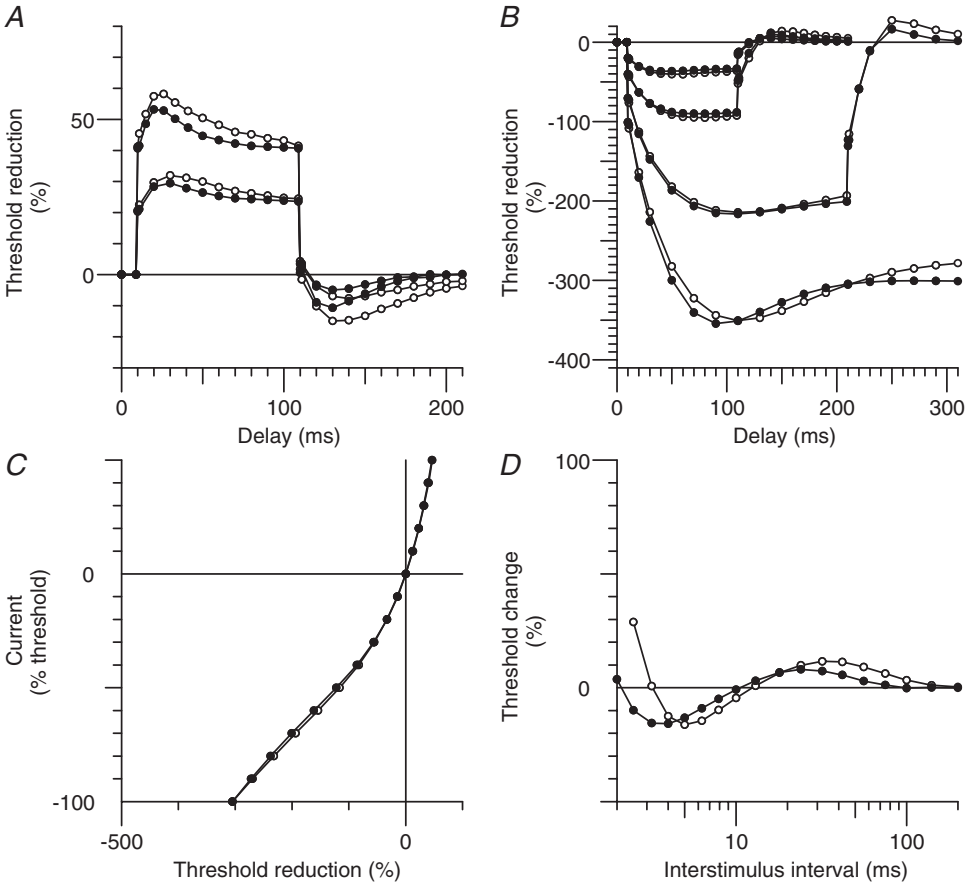

Figure 9. Mathematical model of the hyperthermia-induced changes in excitability of sensory axons
The open circles indicate the Bostock model as modified for sensory axons (Howells *et al.* 2012), and the modelled changes during hyperthermia are shown as closed circles. Hyperthermia was modelled by an increase in temperature of 6°C (with the activation kinetics and maximum conductances increased according to their Q_{10} values; see Methods section), a hyperpolarization of the half-activation voltage of I_h (7 mV) and a small additional depolarizing current of 30 pA. *A*, depolarizing threshold electrotonus for +40% and +20% of the control threshold. *B*, hyperpolarizing threshold electrotonus (−20%, −40%, −70% and −100%). *C*, current–threshold relationship. *D*, the recovery of excitability after a supramaximal stimulus.

channels (a surrogate for RMP) in experiments *in vitro* (e.g. −84 and −86 mV in studies on human sensory axons; Schwarz *et al.* 1995) and well within the likely difference in RMP for human sensory and motor axons (3–4 mV; Howells *et al.* 2012). A larger sample size may have yielded a statistically significant increase in the *unconditioned* threshold during hyperthermia, but the difference is likely to be small. The inability of polarization to restore normal recovery cycles during hyperthermia supports the view that a change in RMP was not the primary driver of the observed excitability changes during hyperthermia. The effects of temperature on channel function are more likely to have a greater impact on excitability and the safety margin (see below) than the small change in RMP.

The recovery cycle

The changes in axonal excitability during hyperthermia affected particularly the recovery cycle, possibly reflecting a disturbance to the finely tuned mechanisms underlying action potential generation and propagation.

Refractoriness. The relative refractory period was shorter and refractoriness was reduced during hyperthermia, findings consistent with studies during cooling (where the opposite changes occur; Burke *et al.* 1999; Moldovan & Krarup, 2004; Maurer *et al.* 2010) or around 'normal' temperatures (Kiernan *et al.* 2001*a*). Diffusion of Na^+ ions would be greater and activation of Na^+ channels would be faster with heating (Fig. 10). These changes would lead to an earlier onset of inactivation, accentuating any changes due to the kinetics of the inactivation gate. The changes in refractoriness are consistent with faster recovery from inactivation of Na^+ channels. However temperature-induced changes in K^+ currents would also affect refractoriness, much as they can superexcitability (see below).

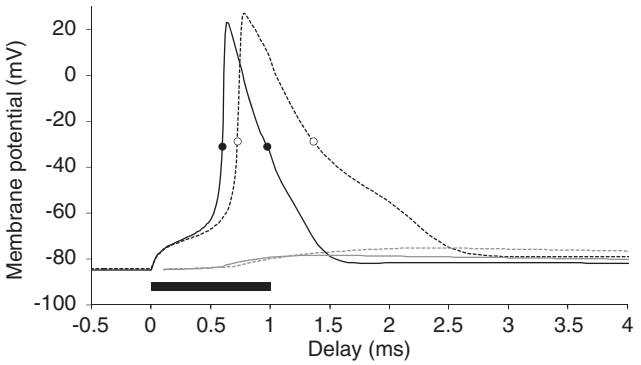

Figure 10. Modelled action potential during hyperthermia
Nodal (black) and internodal (grey) membrane potentials during hyperthermia (continuous lines) and at normal temperature (dashed). Measurements of the half-maximal action potential width were made and are indicated by circles for hyperthermia (0.38 ms; filled) and normal temperature (0.64 ms; open). The filled bar depicts the stimulus duration.

Superexcitability. Superexcitability decreased during hyperthermia, a change unexpected from the earlier studies on human axons. Indeed, when the recovery cycle is normalized to the unconditioned threshold at 'normal' temperatures (dotted lines in Fig. 3*D*), there is only a period of 'relative' superexcitability with a peak that is actually an *increase* in threshold by $+10.3 \pm 8.9\%$. Increased diffusion through the paranodal seal during hyperthermia would serve to *increase* superexcitability. Decreased superexcitability could be due to a narrower action potential (Fig. 10), resulting in reduced charging of the capacitance of the internodal axolemma (Mitrović *et al.* 1993; Honmou *et al.* 1994; Vogel & Schwarz, 1995; Kiernan *et al.* 2001*b*; McIntyre *et al.* 2002; Howells *et al.* 2012), but our modelling suggests that enhanced K^+ currents are more likely to be responsible for the observed changes in superexcitability. By themselves increased diffusion through Na^+ channels (transient and persistent) and their faster kinetics would result in a *wider* action potential, but increases in the potassium currents would provide a dampening effect on the depolarizing after-potential (David *et al.* 1995), counteracting any increases in the Na^+ current. Fig. 10 shows the modelled membrane potential changes for a motor axon during hyperthermia in response to a 1 ms test stimulus. The action potential half-width (measured halfway between RMP and the peak of the action potential) decreased from 0.64 ms to 0.38 ms for normal and hyperthermic temperatures, respectively, corresponding to a Q_{10} of 2.4.

Late subexcitability. The peak of late subexcitability was earlier but its area was not significantly different at hyperthermic temperatures. Late subexcitability reflects after-hyperpolarization due to the decaying activation of K_s channels (Baker *et al.* 1987; Bowe *et al.* 1987; Stys & Waxman, 1994; David *et al.* 1995; Bostock *et al.* 1998). The earlier peak during hyperthermia is probably due to faster K_s kinetics. The lack of difference in the magnitude of late subexcitability may be due to opposing influences on K_s currents: hyperthermia will increase the K_s conductance, but this would hyperpolarize RMP, resulting in a smaller electrochemical gradient for K^+ currents.

Accommodation to long-lasting depolarization

There was no significant difference in the excitability during the first 10 ms of depolarizing threshold electrotonus during hyperthermia and at normal temperatures (Fig. 3*A*), as would be expected if hyperthermia led to faster activation of K_f channels. However Baker and colleagues (1987) have shown that the fast outward rectification

due to K_f currents would occur within the first millisecond at 30°C (see Fig. 5*A* in Baker *et al.* 1987) and presumably faster at warmer temperatures. Additionally, a similar increase in the maximal conductances of Na^+ and K_f channels during hyperthermia could cancel any effect during early depolarizing threshold electrotonus. Increased diffusion through, and faster kinetics of, slow potassium (K_s) channels during hyperthermia can be seen in the faster accommodation to depolarizing currents, sufficient to limit the peak depolarization. The reduced peak depolarization would result in a smaller K_s current and correspondingly a smaller threshold undershoot when the polarizing current ends (Schwarz *et al.* 2006). The primary effect of hyperthermia is on the *kinetics* of K_s, and the current will be enhanced only if the overall depolarization is the same or greater.

The hyperpolarization-activated cation conductance, I_h

Unexpectedly, inward rectification was reduced during hyperthermia (Fig. 3*B*, Table 1). If the diffusion through I_h channels and their activation increase with temperature, one would expect greater inward rectification with heating. The reverse was seen. Our modelling suggests that this apparent paradox can be resolved by hyperpolarization of the voltage dependence of I_h channels and the addition of a small steady depolarizing current. The effects of temperature on the activation kinetics of voltage-gated ion channels have been well studied, but less is known about the effect of temperature on their voltage dependence. However, Hart (1983) reported a similar temperature dependence of the half-activation voltage of the cardiac isoform, I_f, in sheep Purkinje fibres. The voltage dependence of other channels could be similarly altered (Thomas *et al.* 2009), but the present study provides no compelling reasons for postulating such a change. The temperature dependence of HCN channels may involve the voltage sensor directly or indirectly via allosteric activation (Pian *et al.* 2006, 2007; Börjesson & Elinder, 2008). Some regulators of HCN channels can shift the voltage dependence of HCN channels by up to 50 mV (reviewed in Biel *et al.* 2009), and it is likely that the potential modulation of HCN channels is greater than occurs with other channels.

The modelling suggests that the reduced inward rectification seen in Figs 3 and 6 may be accompanied by greater activity of slow internodally located isoforms of I_h. This implies, firstly, that human axons are likely to express more than one HCN isoform, secondly, that current techniques document the properties of only the faster isoform(s) and, thirdly, that hyperthermia may have different effects on different isoforms. We are aware of no data to support the latter speculation.

The role of K^+ channels in hyperthermia

Changes in K_s currents. Changes in K_s currents appear to be a major factor affecting excitability during hyperthermia, responsible for faster accommodation to depolarizing currents, the reduced super- and earlier late sub-excitability and possibly contributing to the shorter RRP, as discussed above. Sittl and colleagues (2010) tested axonal excitability in myelinated axons of rat sural nerve with the K_v7 (K_s) channel opener flupirtine, and reported increased threshold, reduced refractoriness and increased superexcitability, all consistent with hyperpolarization of RMP. In contrast the present study found reduced superexcitability, probably due to faster activation kinetics of both K_f and K_s channels.

Greater access to K_f channels at the paranode during hyperthermia. Increased diffusion through the paranodal seal to the periaxonal space could have an effect on excitability analogous to that of paranodal demyelination or a loosening of the myelin sheath attachment (Cappelen-Smith *et al.* 2001; Nodera *et al.* 2004; Stephanova & Daskalova, 2005). If so this could jeopardize action potential generation, thereby predisposing to conduction block, much as seen in those clinical studies.

Variability of hyperpolarizing threshold electrotonus measures

Tomlinson and colleagues (2010) examined the inter- and intra-subject variability of measures of hyperpolarizing threshold electrotonus and found that despite these measures appearing variable, that they are actually characteristic of an individual. The data in the present study suggests that the variability of hyperpolarizing threshold electrotonus measures is greater in experiments performed on different days than those in the same session. This is perhaps unsurprising given the number of modulators of HCN channel function, but it does have implications for studies which aim to compare hyperpolarizing threshold electrotonus on different occasions.

Clinical implications

The change in excitability in both sensory and motor axons during hyperthermia is the product of several mechanisms, all of which have implications for the security of conduction.

Safety margin and conduction block. Any reduction in the safety margin for action potential generation during hyperthermia may be of functional significance in healthy motor axons (see section on Fatigue below), but is likely to be even more important for already impaired axons.

Our results suggest four mechanisms for a deterioration of the safety margin during hyperthermia. First, at rest, motor axons are probably hyperpolarized 3–4 mV relative to sensory axons (Howells *et al.* 2012), and even slight hyperpolarization during hyperthermia would induce conduction block more readily in motor axons than sensory. Second, the voltage dependence of HCN channels in motor axons is also more hyperpolarized than in sensory axons (Howells *et al.* 2012), and the further hyperpolarization during hyperthermia, would render them less able to counter activity-dependent hyperpolarization, making motor axons even more vulnerable to conduction block. Third, our modelling suggests that faster channel kinetics during hyperthermia will result in a narrower action potential (Fig. 10), such that the time integral of the driving current for the action potential would be reduced. Finally the narrow action potential would result in reduced charging of the internodal axolemma (Fig. 10), affecting superexcitability and the ability to transmit high firing frequencies (see below).

Fatigue. Both central and peripheral mechanisms contribute to the development of fatigue in healthy subjects (Gandevia, 2001) and fatigue can arise from defects at a number of levels in those affected by neuromuscular disease or febrile illness (Friman *et al.* 1977; Thomas & Zijdewind, 2006).

Todd and colleagues (2005) proposed that during hyperthermia achieving maximal force could impose a greater impulse load because a higher motor unit firing frequency would be required to achieve twitch fusion. This would require greater inward rectification to counter the greater activity-dependent hyperpolarization. However the ability to mobilize at least some HCN isoforms underlying I_h appears to be impaired by hyperthermia. As noted above, the reduction in superexcitability seen in the current study may also contribute to the failure of motor axons to achieve transient high firing rates of 50–200 Hz during hyperthermia. This could limit the ability of the motor axon to transmit action potentials at 50–200 Hz through branch points into nerve terminals (Adrian & Lucas, 1912; Swadlow *et al.* 1980; Zhou & Chiu, 2001, Debanne *et al.* 2011). Symptoms of fatigue in neuromuscular disease are often exacerbated by elevated temperatures. Exercise and heat are both recognized triggers of fatigue in sufferers of multiple sclerosis with already impaired safety margins (Uhthoff's sign; Guthrie & Nelson, 1995; Vucic *et al.* 2010), and exercise may accentuate weakness in chronic inflammatory demyelinating polyneuropathy and multifocal motor neuropathy due to the development of activity-dependent conduction block (Cappelen-Smith *et al.* 2000; Kaji *et al.* 2000). Even in amyotrophic lateral sclerosis with primarily lower motor neurone involvement, surviving motor axons may suffer from greater activity-dependent hyperpolarization because they are required to maintain an increased impulse load (Vucic *et al.* 2007).

Fever is a common feature of infectious diseases, such as influenza. Friman and colleagues (1977) reported increased 'jitter' in single-fibre EMG recordings in patients suffering from influenza. They attributed this to hyperthermia-induced blockade of neuromuscular transmission, but the current study provides support for the possibility of branch-point failure due to reduced excitability and a reduction in the safety margin for action potential propagation during hyperthermia.

References

Adrian ED & Lucas K (1912). On the summation of propagated disturbances in nerve and muscle. *J Physiol* **44**, 68–124.

Baker M, Bostock H, Grafe P & Martius P (1987). Function and distribution of three types of rectifying channel in rat spinal root myelinated axons. *J Physiol* **383**, 45–67.

Barrett EF & Barrett JN (1982). Intracellular recording from vertebrate myelinated axons: mechanism of the depolarizing afterpotential. *J Physiol* **323**, 117–144.

Bergmans J. (1970). *The Physiology of Single Human Nerve Fibres*. University of Louvain, Vander, Belgium.

Biel M, Wahl-Schott C, Michalakis S & Zong X (2009). Hyperpolarization-activated cation channels: From genes to function. *Physiol Rev* **89**, 847–885.

Börjesson SI & Elinder F (2008). Structure, function, and modification of the voltage sensor in voltage-gated ion channels. *Cell Biochem Biophys* **52**, 149–174.

Bostock H, Baker M & Reid G (1991). Changes in excitability of human motor axons underlying post-ischaemic fasciculations: evidence for two stable states. *J Physiol* **441**, 537–557.

Bostock H, Cikurel K & Burke D (1998). Threshold tracking techniques in the study of the human peripheral nerve. *Muscle Nerve* **21**, 137–158.

Bowe CM, Kocsis JD & Waxman SG (1987). The association of the supernormal period and the depolarizing afterpotential in myelinated frog and rat sciatic nerve. *Neuroscience* **21**, 585–593.

Buchthal F & Rosenfalck P (1966). Evoked action potentials and conduction velocity in human sensory nerves. *Brain Res* **3**, 1–122.

Burke D, Mogyoros I, Vagg R & Kiernan MC (1999). Temperature dependence of excitability indices of human cutaneous afferents. *Muscle Nerve* **22**, 51–60.

Cappelen-Smith C, Kuwabara S, Lin CS, Mogyoros I & Burke D (2000). Activity-dependent hyperpolarization and conduction block in chronic inflammatory demyelinating polyneuropathy. *Ann Neurol* **48**, 826–832.

Cappelen-Smith C, Kuwabara S, Lin CS, Mogyoros I & Burke D (2001). Membrane properties in chronic inflammatory demyelinating polyneuropathy. *Brain* **124**, 2439–2447.

David G, Modney G, Scappaticci KA, Barrett JN & Barrett EF (1995). Electrical and morphological factors influencing the depolarizing after-potential in rat and lizard myelinated axons. *J Physiol* **489**, 141–157.

Davis FA, Schauf CL, Reed BJ, Kesler RL (1975). Experimental studies of the effects of extrinsic factors on conduction in normal and demyelinated nerve. 1. Temperature. *J Neuro Neurosurg Psychiatry* **39**, 442–448.

Debanne D, Campanac E, Bialowas A, Carlier E & Alcaraz G (2011). Axon physiology. *Physiol Rev* **91**, 555–602.

Frankenhaeuser B & Moore LE (1963). The effect of temperature on the sodium and potassium permeability changes in myelinated nerve fibres of *Xenopus laevis*. *J Physiol* **169**, 431–437.

Friman G, Schiller HH & Schwartz MS (1977). Distubed neuromuscular transmission in viral infections. *Scand J Infect Dis* **9**, 99–103.

Gandevia, SC (2001). Spinal and supraspinal factors in human muscle fatigue. *Physiol Rev* **81**, 1725–1789.

Guthrie TC & Nelson DA (1995). Influence of temperature on multiple sclerosis: critical review of mechanisms and research potential. *J Neurol Sci* **129**, 1–8.

Guttman R (1971). The effect of temperature on the function of excitable membranes. In *Biophysics and Physiology of Excitable Membranes*. ed. Adelman WJ Jr, pp 320–336. Van Nostrand Reinhold, New York.

Hart G (1983). The kinetics and temperature dependence of the pace-maker current i_f in sheep Purkinje fibres. *J Physiol* **337**, 401–416.

Hille B (1992). *Ionic Channels of Excitable Membranes*. 2nd edn. Sinauer Associates, Sunderland, MA, USA.

Hodgkin AL & Katz B (1949). The effect of temperature on the electrical activity of the giant axon of the squid. *J Physiol* **109**, 240–249.

Hodgkin AL & Huxley AF (1952*a*). The dual effect of membrane potential on sodium conductance in the giant axon of *Loligo*. *J Physiol* **116**, 497–506.

Hodgkin AL & Huxley AF (1952*b*). A quantitative description of membrane current and its application to conduction and excitation in nerve. *J Physiol* **117**, 500–544.

Hodgkin AL, Huxley AF & Katz B (1952). Measurement of current–voltage relations in the membrane of the giant axon of *Loligo*. *J Physiol* **116**, 424–448.

Honmou O, Utzschneider DA, Rizzo MA, Bowe CM, Waxman SG & Kocsis JD (1994). Delayed depolarization and slow sodium currents in cutaneous afferents. *J Neurophysiol* **71**, 1627–1637.

Howells J, Trevillion L, Bostock H & Burke D (2012). The voltage dependence of I_h in human myelinated axons. *J Physiol* **590**, 1625–1640.

Jankelowitz SK, Howells J & Burke D (2007). Plasticity of inwardly rectifying conductances following a corticospinal lesion in human subjects. *J Physiol* **581**, 927–940.

Kaji R, Bostock H, Kohara N, Murase N, Kimura J & Shibasaki H (2000). Activity-dependent conduction block in multifocal motor neuropathy. *Brain* **123**, 1602–1611.

Kiernan MC & Bostock H (2000). Effects of membrane polarization and ischaemia on the excitability properties of human motor axons. *Brain* **123**, 2542–2551.

Kiernan MC, Burke D, Andersen KJ & Bostock H (2000). Multiple measures of axonal excitability: A new approach in clinical testing. *Muscle Nerve* **23**, 399–409.

Kiernan MC, Cikurel K & Bostock H (2001a). Effects of temperature on the excitability properties of human motor axons. *Brain* **124**, 816–825.

Kiernan MC, Isbister GK, Lin CS-Y, Burke D & Bostock H (2005). Acute Tetrodotoxin-induced neurotoxicity after ingestion of puffer fish. *Ann Neurol* **57**, 339–348.

Kiernan MC, Lin CS-Y, Andersen KV, Murray NMF & Bostock H (2001b). Clinical evaluation of excitability measures in sensory nerve. *Muscle Nerve* **24**, 883–892.

Krishnan AK, Lin CS-Y, Park SB & Kiernan MC (2009). Axonal ion channels from bench to bedside: A translational neuroscience perspective. *Prog Neurobiol* **89**, 288–313.

Lin CS-Y, Krishnan AV, Lee M-J, Zagami AS, You H-L, Yang C-C, Bostock H & Kiernan MC (2008). Nerve function and dysfunction in acute intermittent porphyria. *Brain* **131**, 2510–2519.

Ludin HP & Beyeler F (1977). Temperature dependence of normal sensory nerve action potentials. *J Neurol* **216**, 173–180.

McIntyre CC, Richardson G & Grill WM (2002). Modeling the excitability of mammalian nerve fibers: influence of afterpotentials on the recovery cycle. *J Neurophysiol* **87**, 995–1006.

Maurer K, Wacker J, Vastani N, Seifert B & Spahn DR (2010). Changes in axonal excitability of primary sensory afferents with general anaesthesia in humans. *Brit J Anaesth* **105**, 648–656.

Mierzwa A, Shroff S & Rosenbluth J (2010). Permeability of the paranodal junction of myelinated nerve fibers. *J Neurosci* **30**, 15962–15968.

Mitrović N, Quasthoff S & Grafe P (1993). Sodium channel inactivation kinetics of rat sensory and motor nerve fibres and their modulation by glutathione. *Pflugers Arch* **425**, 453–461.

Mogyoros I, Kiernan MC, Burke D (1996). Strength–duration properties of human peripheral nerve. *Brain* **119**, 439–447.

Moldovan M & Krarup C (2004). Mechanisms of hyperpolarization in regenerated mature motor axons in cat. *J Physiol* **560**, 807–819.

Moore JW (1958). Temperature and drug effects on squid axon membrane ion conductances. *Fed Proc* **17**, 113.

Ng K, Howells J, Pollard JD & Burke D (2008). Up-regulation of slow K^+ channels in peripheral motor axons: a transcriptional channelopathy in multiple sclerosis. *Brain* **131**, 3062–3071.

Nodera H, Bostock H, Kuwabara S, Sakamoto T, Asanuma K, Jia-Ying S, Ogawara K, Hattori N, Hirayama M, Sobue G & Kaji R (2004). Nerve excitability properties in Charcot-Marie-Tooth disease type 1A. *Brain* **127**, 203–211.

Palti Y & Adelman WJ Jr (1969). Measurement of axonal membrane conductances and capacity by means of a varying potential control voltage clamp. *J Membrane Biol* **1**, 431–458.

Pian P, Bucchi A, DeCostanzo A, Robinson RB & Siegelbaum SA (2007). Modulation of cyclic nucleotide-regulated HCN channels by PIP2 and receptors coupled to phospholipase C. *Pflugers Arch* **455**, 125–145.

Pian P, Bucchi A, Robinson RB & Siegelbaum SA (2006). Regulation of gating and rundown of HCN hyperpolarization-activated channels by exogenous and endogenous PIP2. *J Gen Physiol* **128**, 593–604.
Rasminsky M (1973). The effects of temperature on conduction in demyelinated single nerve fibers. *Arch Neurol* **28**, 287–292.
Rutkove SB (2001). Effects of temperature on neuromuscular electrophysiology. *Muscle Nerve* **24**, 867–882.
Rutkove SB, Kothari MJ & Shefner JM (1997). Nerve, muscle, and neuromuscular junction electrophysiology at high temperature. *Muscle Nerve* **20**, 431–436.
Schauf CL & Davis FA (1974). Impulse conduction in multiple sclerosis: a theoretical basis for modification by temperature and pharmacological agents. *J Neurol Neurosurg Psychiatry* **37**, 152–161.
Schwarz JR & Eikhof G (1987). Na currents and action potentials in rat myelinated nerve fibres at 20 and 37°C. *Pflugers Arch* **409**, 569–577.
Schwarz JR, Glassmeier G, Cooper EC, Kao TC, Nodera H, Tabuena D, Kaji R & Bostock H (2006). KCNQ channels mediate IKs, a slow K^+ current regulating excitability in the rat node of Ranvier. *J Physiol* **573**, 17–34.
Schwarz JR, Reid G & Bostock H (1995). Action potentials and membrane currents in the human node of Ranvier. *Pflugers Arch* **430**, 283–292.
Sittl R, Carr RW, Schwarz JR & Grafe P (2010). The Kv7 potassium channel activator flupirtine affects clinical excitability parameters of myelinated axons in isolated rat sural nerve. *J Peripher Nerv Sys* **15**, 63–72.
Stephanova DI & Daskalova M (2005). Differences in potentials and excitability properties in simulated cases of demyelinating neuropathies. Part II. Paranodal demyelination. *Clin Neurophysiol* **116**, 1159–1166.
Stys PK & Waxman SG (1994). Activity-dependent modulation of excitability: implications for axonal physiology and pathophysiology. *Muscle Nerve* **17**, 969–974.
Swadlow HA, Kocsis JD & Waxman SG (1980). Modulation of impulse conduction along the axonal tree. *Ann Rev Biophys Bioeng* **9**, 143–179.
Tasaki I (1955). New measurements of the capacity and the resistance of the myelin sheath and the nodal membrane of the isolated frog nerve fibre. *Am J Physiol* **181**, 639–650.
Taylor RE & Chandler WK (1962). Effect of temperature on squid axon membrane capacity. *Biophys Soc Abstr* TD1.
Thomas CK & Zijdewind I (2006). Fatigue of muscles weakened by death of motoneurons. *Muscle Nerve* **33**, 21–41.
Thomas EA, Hawkins RJ, Richards KL, Xu R, Gazina EV & Petrou S (2009). Heat opens axon initial segment sodium channels: A febrile seizure mechanism? *Ann Neurol* **66**, 219–226.
Todd G, Butler JE, Taylor JL & Gandevia SC (2005). Hyperthermia: a failure of the motor cortex and the muscle. *J Physiol* **563**, 621–631.
Tomlinson S, Burke D, Hanna M, Koltzenburg M & Bostock H (2010). In vivo assessment of HCN channel current (I_h) in human motor axons. *Muscle Nerve* **41**, 247–256.
Vogel W & Schwarz JR (1995). Voltage-clamp studies in axons: macroscopic and single-channel currents. In *The Axon*, ed. Waxman SG, Kocsis JD, Stys PK, pp 257–280. Oxford University Press, New York.
Vucic S, Burke D & Kiernan MC (2010). Fatigue in multiple sclerosis: mechanisms and management. *Clin Neurophysiol* **121**, 809–817.
Vucic S, Krishnan AV & Kiernan MC (2007). Fatigue and activity dependent changes in axonal excitability in amyotrophic lateral sclerosis. *J Neurol Neurosurg Psychiatry* **78**, 1202–1208.
Zhou L & Chiu SY (2001). Computer model for action potential propagation through branch point in myelinated nerves. *J Neurophysiol* **85**, 197–210.

Additional information

Competing interests

None declared.

Author contributions

J.H., D.C. and D.B. contributed to the study design. J.H., D.C. and L.T. collected and analysed the data. J.H. and L.T. performed the mathematical modelling. All authors contributed to the interpretation of the data and the preparation of the manuscript and have approved the final version. The experiments were performed at The University of Sydney.

Funding

This research was supported by the National Health and Medical Research Council of Australia. D.C. was supported by a stipend from the Deutsche Gesellschaft für Klinische Neurophysiologie.

Acknowledgements

The authors wish to thank Adelle Coster and Hans Coster for valuable discussions during the preparation of the manuscript.